

MUSMAR BASED SWITCHING CONTROL OF A SOLAR COLLECTOR FIELD

L. Rato*, D. Borrelli†, E. Mosca‡, J. M. Lemos§, P. Balsa¶

**INESC, R. Alves Redol 9, Apartado 13069, 1017 Lisboa, Portugal,
Fax +351.1.3145843, email: Luis.Rato@inesc.pt,*

†*Università di Firenze, DSI, Via S. Marta 3, 50139 Firenze, Italy,
Fax +39.55.4796363, email: donato@dsi.dsi.unifi.it*

‡*DSI, Fax +39.55.4796363, email: mosca@dsi.dsi.unifi.it*

§*INESC/IST, Fax +351.1.3145843 email: Joao.Lemos@inesc.pt*

¶*PSA, Fax: +34.50.365015, email: pedro@psazp.psa.es*

Keywords : Switching control, adaptive control, predictive control, solar energy.

Abstract

This paper presents a switching controller for the distributed collector field of a solar power plant. The switching control strategy has been used to cope with the changes in plant dynamic behavior induced by different operating conditions. The underlying predictive models and controllers were designed using the MUSMAR adaptive algorithm. Experimental results obtained at *Plataforma Solar de Almeria* (in Spain), are presented.

1 Introduction

This paper is concerned with the application of switching control to the regulation of the outlet oil temperature of a distributed solar collector field. This is achieved by adjusting the oil flow. The change of the flow leads to significant changes in plant dynamic behaviour which has to be compensated.

Several control schemes have been successfully applied to this solar collector field including a pole-placement self-tuner [2], MUSMAR adaptive control [4, 5], fuzzy control [11], gain-scheduling GPC [1], and a prescheduled resonance cancellation [9],

In this paper a switching control strategy [7] is used to cope with the fast changes in the dynamic behaviour. The MUSMAR adaptive algorithm [6] is applied to design the controllers, considering the properties of this algorithm

as far as nonlinearities and unmodeled dynamics are concerned.

The paper is organized as follows: section 2 briefly presents the ACUREX solar collector field; in section 3 the control algorithm is described, in section 4 some test results are presented; and section 5 presents the conclusions.

2 Description of the Solar Collector Field

The ACUREX distributed solar collector field used in the experiments described in this paper is well described in readily available literature [2, 3, 12].

The field consists of 480 parabolic mirrors arranged in 20 East-West oriented rows to form 10 parallel loops. Each loop is 172 m long, where 142 m are exposed to the radiation while the remaining 30 m are passive. The total aperture surface is 2672 m². The plant is able to provide 1.2 MW peak of thermal power. The parabolic mirrors concentrate the radiation in a steel pipe heating a heat transfer medium is Santotherm 55 synthetic oil. The oil is pumped from the bottom of a storage tank through the field till the top of the tank. This oil has good thermal conductivity and a density highly dependent on the temperature. This property leads to a stratification in the tank, with the hottest oil in the top of the tank and the coldest in the bottom.

An one-axis independent tracking system for each group of collectors allows following the varying elevation of the sun during the course of the day.

The oil pump is connected to a PID controller regulating the flow through the field, the oil flow being the manipulated variable. The main goal of the control system is

*Supported by JNICT under Grant PRAXIS XXI BD/2747/94

to regulate the outlet field oil temperature at a constant level. The main disturbances are solar radiation and inlet oil temperature.

3 Control Algorithm

Around each operating point defined by the values of oil flow and radiation the plant is assumed to be modeled by a discrete time SISO linear time-invariant system. A linear controller, designed in a way to be precised below, is associated to each of the above models. Fig.(1) depicts a block diagram of the feedback control loop as defined around one operating point. The following notation is used:

- y denotes the average temperature of the oil at the outlet of the collector field loops.
- u denotes the oil flow (manipulated variable).
- δu denotes increments of u .
- y^* denotes the reference to be tracked by y .
- $k_\sigma(q)$ denotes the transfer function of the σ -th controller.
- ν_p denotes the transfer function of the candidate p -th model.

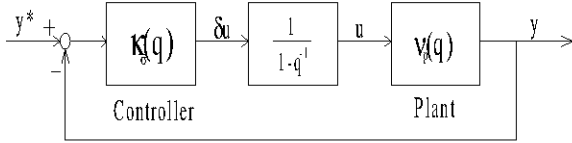


Figure 1: Feedback loop with the integrator.

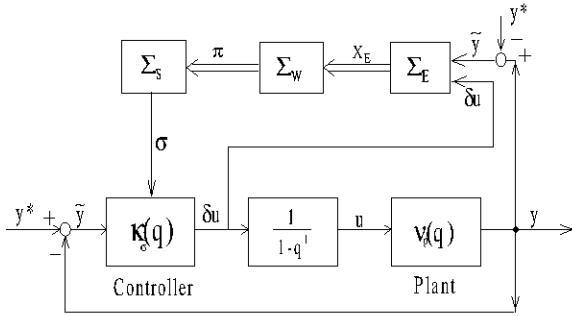


Figure 2: Feedback control loop and the supervisor.

In the above, q denotes the forward shift operator. An integrator has been included in the loop, in series with the controller, in order to ensure zero steady-state position error. When the plant operating condition, as defined by the flow and the radiation values, change, the index p of the

candidate model $\nu_p(q)$ also changes. Thus, the controller should be provided with a mechanism which adjusts the index σ of the active controller transfer function, $k_\sigma(q)$, in order to match the operating conditions. Fig.2 depicts one such mechanism, connected to the closed-loop system, which will hereafter be referred as the *supervisor*.

3.1 The Supervisor

The supervisor used in this paper follows the structure proposed in [8, 7] and is detailed in fig.3. It consists of three stages:

- A shared-state estimator, Σ_E .
- A performance weight generator, Σ_W .
- A switching logic scheme, Σ_S .

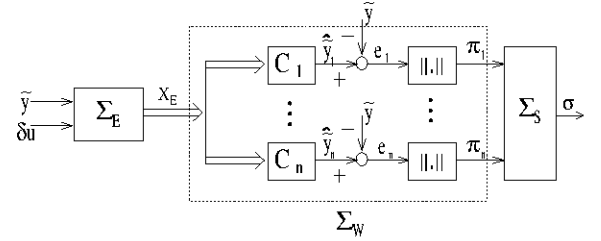


Figure 3: Shared-state estimator based supervisor.

The shared-state estimator generates a vector X_E to be used by a bank of models, each corresponding to one operating point. It is defined by

$$X_E(t+1) = \begin{bmatrix} A_E & 0 \\ 0 & A_E \end{bmatrix} X_E(t) +$$

$$\begin{bmatrix} b_E \\ 0 \end{bmatrix} y(t) + \begin{bmatrix} 0 \\ b_E \end{bmatrix} \delta u(t) \quad (1)$$

$$\hat{y}_p = C_p X_E(t) \quad (2)$$

where A_E and b_E are given by

$$A_E = \begin{bmatrix} 0 & 0 & 0 & 0 & \dots \\ 1 & 0 & 0 & 0 & \dots \\ 0 & 1 & 0 & 0 & \dots \\ 0 & 0 & 1 & 0 & \dots \\ \vdots & \vdots & \ddots & \ddots & \ddots \end{bmatrix} \quad b_E = \begin{bmatrix} 1 \\ 0 \\ 0 \\ 0 \\ \vdots \end{bmatrix} \quad (3)$$

and C_p depends on the plant model p parameters.

One of the possible choices for the performance weight generator is the integral of the square errors of the estimates. A low pass filter of the estimator errors is obtained by

$$\pi_i(t+1) = \pi_i(t)\lambda + (\hat{y}_i - \tilde{y})^2 \quad (4)$$

where $\lambda < 1$ and π_i is the performance signal associated to the i -th nominal process model. In this paper a $\lambda = 0.9$ is used. The lower π_i , the better the matching between the i -th model and the operating conditions. The switching logic scheme used in this paper is defined in fig.4. This algorithm switches among controllers, choosing one with the lowest performance signal, and assuring a minimum period of time between each switch. This period of time is referred as the *dwell time*, and has been settled as 10.

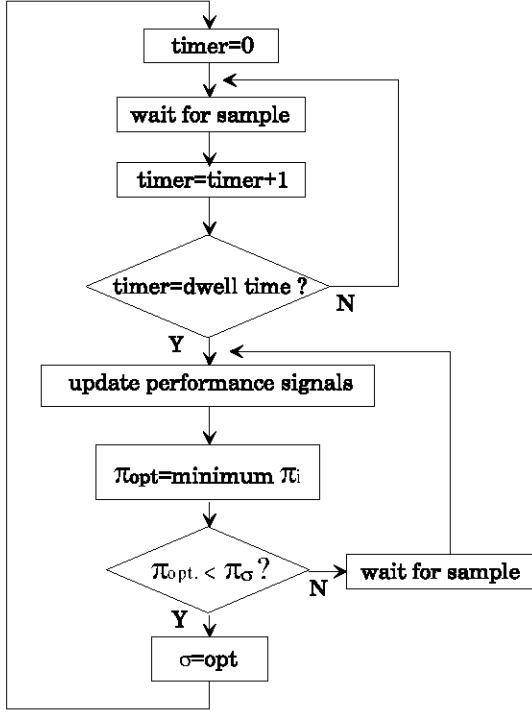


Figure 4: Switching logic algorithm.

3.2 Controller Design

Several methods can be used to design the linear controllers $k_\sigma(q)$, matching each of the operating conditions. In this paper the MUSMAR adaptive control algorithm is applied of-line to each of the candidate models $\nu_p(q)$ and run till convergence is obtained. The resulting controller gains are then recorded, defining $k_p(q)$.

Consider a SISO ARMAX plant

$$A(q^{-1})y(t) = B(q^{-1})\delta u(t-1) + C(q^{-1})e(t) \quad (5)$$

where $y(t)$ is the output, $\delta u(t)$ is the input, $e(t)$ is a zero mean uncorrelated independent distribution, and $A(q^{-1})$, $B(q^{-1})$, $C(q^{-1})$ are polynomials such that A and B have no unstable common factors. Polynomial C is strictly minimum phase and A , B , and C do not share any unstable common factors. Associate to this plant the quadratic

cost functional defined over a T -steps horizon:

$$J_T(t) = \frac{1}{T} E \left\{ \sum_{k=t}^{t+T-1} [\tilde{y}^2(k+1) + \rho \delta u^2(k) | I(t)] \right\} \quad (6)$$

where ρ is a weight in the control action, $\tilde{y}(t)$ is the tracking error,

$$\tilde{y}(t) = y(t) - y^*(t) \quad (7)$$

and $E \{ \cdot | I(t) \}$ denotes the mean conditioned on the information available up to time t (projection)[10]. The basic MUSMAR optimization problem [6] is formulated as follows: given the sequence of constant feedback gains

$$\{F_0, F_0, F_0, \dots\} \quad (8)$$

operating in the plant from $t+1$ up to $t+T-1$, find the feedback gain vector, F , such that

$$\delta u(t) = F' s(t) \quad (9)$$

$$s(t) = [\tilde{y}(t) \ \tilde{y}(t-1) \ \dots \ \tilde{y}(t-n_a+1)$$

$$\delta u(t-1) \ \delta u(t-2) \ \dots \ \delta u(t-n_b)]' \quad (10)$$

minimizes the cost functional $J_T(t)$. This strategy can be adaptively implemented as follows

MUSMAR Algorithm[6]

1. Compute the recursive-least-square (RLS) estimate of the parameters θ_i , ψ_i , μ_i and ϕ_i in the predictive models

$$\tilde{y}(t+i-T) \approx \theta_i \delta u(t-T) + \psi_i' s(t-1) \quad (11)$$

$$\delta u(t+i-T-1) \approx \mu_{i-1} \delta u(t-T) + \phi_{i-1}' s(t-1) \quad (12)$$

$$i = 1 \dots T$$

where \approx denotes equality in least squares sense.

2. Update the feedback gains according to

$$F = - \frac{\sum_{i=1}^T \theta_i \psi_i + \rho \sum_{i=1}^{T-1} \mu_i \phi_i}{\sum_{i=1}^T \theta_i^2 + \rho(1 + \sum_{i=1}^{T-1} \mu_i^2)} \quad (13)$$

and calculate the control signal by

$$\delta u(t) = F' s(t) + \eta(t) \quad (14)$$

where $\eta(t)$ is a white noise dither signal injected in order to fulfill a persistency of excitation condition and $s(t)$ is as in (10) being a sufficient statistic to compute the control, hereafter referred as the *pseudostate*.

Consider the 1 step ahead predictive model of the plant.

$$\hat{\tilde{y}}_i(t) = [\theta_i \ \psi_i'] [\delta u(t-1) \ s'(t-1)]' \quad (15)$$

and let the parameter vector c_i in (2) and the shared state $X_E(t)$ be

$$c_i = [\theta_i \ \psi_i] \quad (16)$$

$$X_E(t) = [\delta u(t-1) \ s(t-1)]' \quad (17)$$

The estimator error is defined as the one step ahead prediction error

$$e_i = \tilde{y}_i(t) - \hat{\tilde{y}}_i(t) = \tilde{y}_i(t) - [\theta_i \ \psi_i][\delta u(t-1) \ s(t-1)]' \quad (18)$$

and the control signal candidates are

$$\delta u_i(t) = L'_i s(t) \quad (19)$$

where L_i is the i -th candidate for the controller parameters obtained with the MUSMAR algorithm, i.e. L_i is obtained by running MUSMAR with a model of the plant while the i -th combination of flow and radiation is kept constant. The dynamic behavior of the system depends mainly on the flow through the field (the manipulated variable). The influence from the radiation can be roughly described as a change in the static gain of the system. Thus, linear models were identified from experimental data in two different operating conditions:

- 1 model with the flow around 5 l/s: model no. 0.
- 2 models with the flow around 7 l/s obtained with different values of radiation: models no. 4 and 7.

From the above models, other models were obtained multiplying their static gain by a constant C . It is, thus, pos-

Model no.	Flow	C	ρ
0	5 l/s	1.00	100
1	5 l/s	1.50	100
2	5 l/s	0.66	50
3	5 l/s	0.33	10
4	7 l/s	1.00	70
5	7 l/s	1.50	150
6	7 l/s	1.50	150
7	7 l/s	1.00	100

Table 1: Models defined in two operating conditions.

Model no.	Flow	C	ρ
8	3.5 l/s	1.00	1000

Table 2: Model defined with flow 3.5 l/s.

sible to cope with changes on the radiation. In this way models 1, 2, and 3, were obtained from model 0; model 5, from 4; and model 6 from 7. The models are described in table 1. The sampling time has been settled as $T_S = 30$ s. Another model has been identified with the flow around 3.5 l/s and used in the test of 19th July.

The adaptive MUSMAR algorithm has been run with each model, with the structure of the pseudostate defined

by $n_a = 3$ and $n_b = 2$. The prediction horizon has been chosen to be $T = 10$. The values of ρ used with each model are shown in tables 1 and 2

4 Experimental Results

The tests were performed in the ACUREX field, at *Plataforma Solar de Almeria*. Figs. 5 to 8 depict the results obtained in experiments 1 and 2 performed, respectively, in 10 and 11 July 1996.

The graphics show the time evolution of the plant variables since start-up. The temperature reference was chosen as a sequence of positive and negative steps. Apart from the variation due to the daily movement of the sun, there were no other disturbances in radiation. In exper-

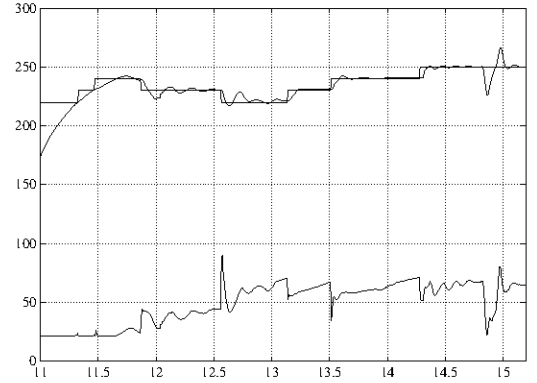


Figure 5: Experiment 1: Reference, output, and $flow \times 10$.

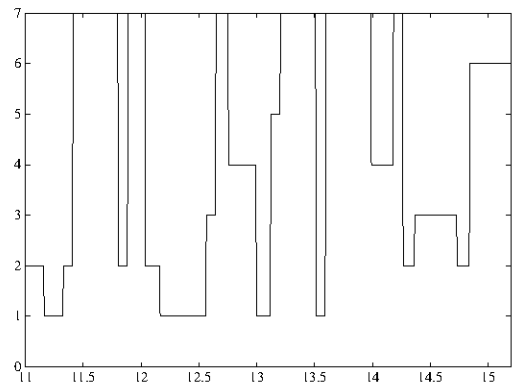


Figure 6: Experiment 1: Supervisor output, σ .

iment 1 about 14h45m the field was lead to stow (defocused) and then recovered. For values of the flow higher than 6 l/s, there is almost no overshoot and the rise time is about 6 minutes. For lower values of the flow, the response

is more oscillatory and the rise time increases. This is so, because the higher the flow the smaller is the residence time of the oil in the field, thus decreasing the effect of the resonant/anti-resonant modes [9].

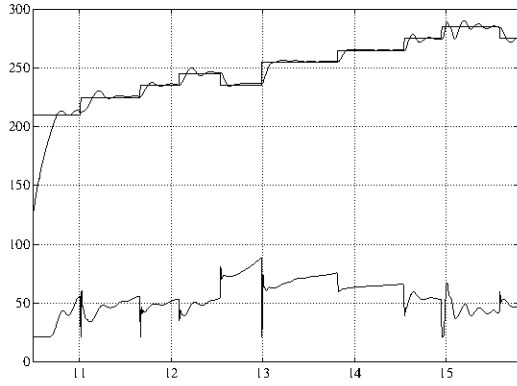


Figure 7: Experiment 2: Reference, output, and $flow \times 10$.

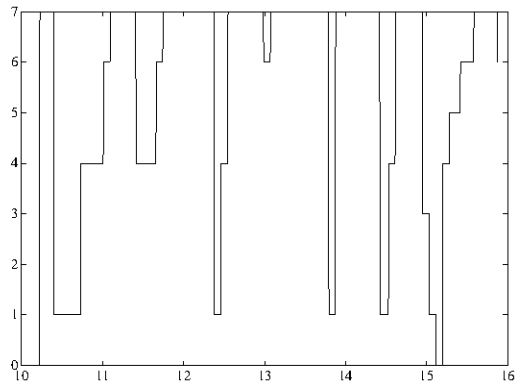


Figure 8: Experiment 2: Supervisor output, σ .

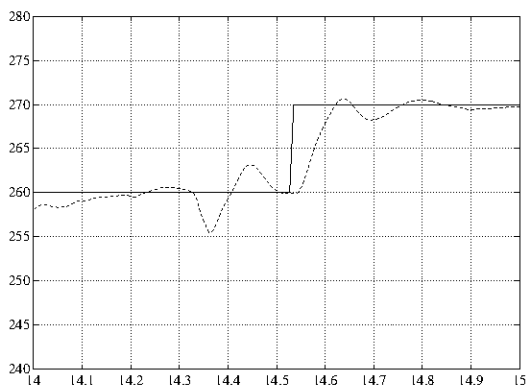


Figure 9: Experiment 3: Reference and output.

Experiment 3 was performed on 15 July 1996. Part of the results are shown in figs.9 to 11. It illustrates the

response of the controller to a fast and strong disturbance in the primary energy source (solar radiation) caused by a cloud.

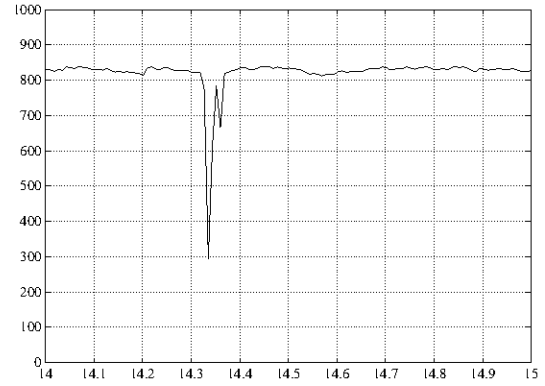


Figure 10: Experiment 3: Solar radiation.

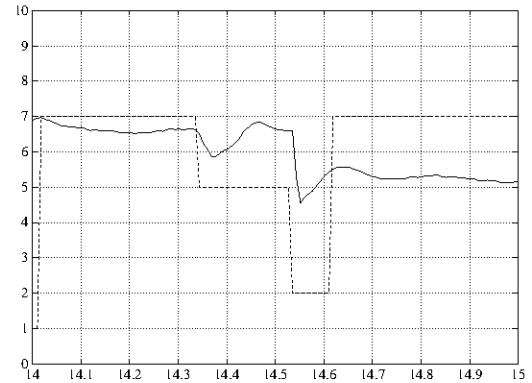


Figure 11: Experiment 3: Supervisor output, σ , and flow.

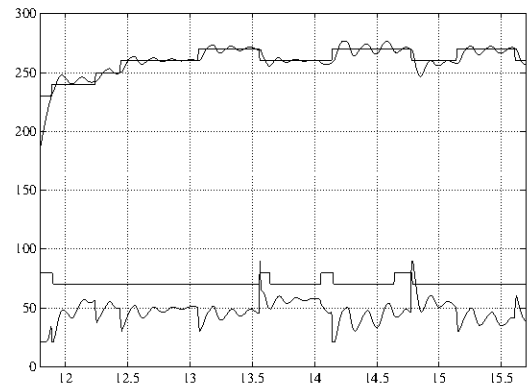


Figure 12: Experiment 4: Reference, output, $\sigma \times 10$, and $flow \times 10$.

Experiment 4 was performed on 19 July 1996. The results can be seen in fig.12. In this experiment only two controllers were used. These are n.7 and n.8 in (table 2). Despite that controller no. 7 is often elected by the switching mechanism in the previous experiments, a feature which also happens here, the resulting performance in this case is poor, due to a persistent oscillatory behavior. This illustrates the importance of the use of a number of controllers covering the various operating conditions.

5 Conclusions

This paper presents experimental results on the application of switching control to a distributed collector solar field. The control structure used consists in a bank of candidate controllers and a supervisor. Each of the candidate controllers is tuned in order to match a region in the plant operating conditions. For that sake, the MUSMAR adaptive controller is applied off-line to a plant model corresponding to the operating condition considered. The candidate controller gains are obtained as the MUSMAR convergence gains. Thus, each candidate controller approximates a steady-state (infinite-horizon) linear quadratic reduced complexity controller.

The supervisor follows the structure proposed in [8, 7] and consists of a shared-state estimator, a performance weight generator and a dwell time switching logic scheme. It elects the active controller by choosing the one corresponding to the predictive model which best fits plant model.

Experimental results are reported assessing the performance of this control strategy and illustrating the improvements achievable by the use of various controllers with respect to the use of just one controller.

Acknowledgment:

All the experiments described in this paper were carried out within the project "Innovative Training Horizons in Applied Solar Thermal and Chemical Technologies" (C.N: ERBFMGECT950023) supported by the European Union Program "Training and Mobility of Researchers" and Promoted by CIEMAT-IER.

References

- [1] Camacho, E. and M. Berenguel. "Application of generalized predictive control to a solar power plant", *Proc. Conf. Advances in Model-Based Predictive Control*, Oxford University, UK, September (1993).
- [2] Camacho, E.; F. R. Rubio and F.M. Hughes M. "Self-Tuning Control of a Solar Power Plant with a Distributed Collector Field", *IEEE control Systems*, April (1992).
- [3] Camacho, E.; F. R. Rubio and J. A. Gutierrez, "Modelling and simulation of a solar power plant with distributed collector system", *IFAC Symp. on Power Systems Modelling and Control Applications*, Brussels, (1988).
- [4] Coito F.; J. M. Lemos, R. N. Silva, E. Mosca, "Adaptive Control of a Solar Energy Plant: Exploiting Accessible Disturbances", *Int. J. of Adaptive Control & Signal Processing*, Vol 11, n.2, (1997)
- [5] Silva, R. N., L. Rato, J. L. Lemos, F Coito. "Cascade control of a distributed Collector Solar Field", *J. of Process Control*, Vol 7, n.2, pag 111-117, (1997).
- [6] Greco, C.; G. Menga; E. Mosca and G. Zappa. "Performance Improvements of Self-tuning Controllers by Multistep Horizons: The MUSMAR Approach", *Automatica*, vol 20, pag 681-699, (1984).
- [7] Morse, A.S.; "Control Using Logic-Based Switching" in "Trends in Control- an European Perspective", A. Isidori (edt.), *Springler-Verlag*, (1995).
- [8] Borrelli, D.; A.S. Morse, E. Mosca "Discrete-Time Supervisory Control of Families of 2-Degree of Freedom Linear Set-Point Controllers", Submitted, Dipartimento de Sistemi e Informatica, Università di Firenze, April (1996).
- [9] Meaburn, A.; F. M. Hughes "Prescheduled Adaptive Control Scheme for Resonance Cancellation of a Distributed solar Collector field" *Solar Energy*, Vol 52, n.2, pag 155-166, (1994)
- [10] Mosca, E., "Optimal Predictive and Adaptive Control", *Prentice-Hall* (1995).
- [11] Rubio, F. R.; M. Berenguel, E. Camacho. "Fuzzy Logic Control of a Solar Power Plant", *IEEE Trans. Fuzzy Systems*, Vol 3, n.4, 459-468, (1995).
- [12] Kaltz, A. "Distributed Collector System Plant Construction Report", IEA/SSPS Operating Agent. *DFVLR*, Cologne, (1982).
- [13] Sanchez, M.; M. Becker (Edt.) "Solar Thermal Test Facilities" Ref. SolarPACES Technical Report III-5/95, (1995)